The Journal of Experimental Medicine

Adult Langerhans cells derive predominantly from embryonic fetal liver monocytes with a minor contribution of yolk sac–derived macrophages

Guillaume Hoeffel,[1] Yilin Wang,[1] Melanie Greter,[2,3] Peter See,[1] Pearline Teo,[1] Benoit Malleret,[1] Marylène Leboeuf,[2,3] Donovan Low,[1] Guillaume Oller,[1] Francisca Almeida,[1] Sharon H.Y. Choy,[4] Marcos Grisotto,[5] Laurent Renia,[1] Simon J. Conway,[6] E. Richard Stanley,[7] Jerry K.Y. Chan,[8,9,10] Lai Guan Ng,[1] Igor M. Samokhvalov,[11] Miriam Merad,[2,3] and Florent Ginhoux[1]

[1]Singapore Immunology Network, Agency for Science, Technology and Research (A*STAR), Immunos Building #3-4, BIOPOLIS, 138648, Singapore
[2]Department of Gene and Cell Medicine and [3]The Immunology Institute, Mount Sinai School of Medicine, New York, NY 10029
[4]Biological Resource Centre, A*STAR, #07-01 Centros, 138668, Singapore
[5]Centro Universitário do Maranhão – UNICEUMA, São Luis, MA, Brazil
[6]Herman B Wells Center for Pediatric Research, Indiana University School of Medicine, Indianapolis, IN 46202
[7]Department of Developmental and Molecular Biology, Albert Einstein College of Medicine, Bronx, NY 10461
[8]Experimental Fetal Medicine Group, Yong Loo Lin School of Medicine, National University of Singapore, 119228 Singapore
[9]Reproductive Medicine, KK Women's and Children's Hospital, 229899 Singapore
[10]Cancer and Stem Cell Biology Program, Duke-NUS Graduate Medical School, 169857 Singapore
[11]Laboratory for Stem Cell Biology, Center for Developmental Biology, Institute of Physical and Chemical Research Kobe, Kobe 6500047, Japan

Langerhans cells (LCs) are the dendritic cells (DCs) of the epidermis, forming one of the first hematopoietic lines of defense against skin pathogens. In contrast to other DCs, LCs arise from hematopoietic precursors that seed the skin before birth. However, the origin of these embryonic precursors remains unclear. Using in vivo lineage tracing, we identify a first wave of yolk sac (YS)–derived primitive myeloid progenitors that seed the skin before the onset of fetal liver hematopoiesis. YS progenitors migrate to the embryo proper, including the prospective skin, where they give rise to LC precursors, and the brain rudiment, where they give rise to microglial cells. However, in contrast to microglia, which remain of YS origin throughout life, YS-derived LC precursors are largely replaced by fetal liver monocytes during late embryogenesis. Consequently, adult LCs derive predominantly from fetal liver monocyte-derived cells with a minor contribution of YS-derived cells. Altogether, we establish that adult LCs have a dual origin, bridging early embryonic and late fetal myeloid development.

CORRESPONDENCE
Florent Ginhoux:
florent_ginhoux@
immunol.a-star.edu.sg
OR
Miriam Merad:
miriam.merad@mssm.edu

Abbreviations used: 4'OHT, 4-hydroxytamoxifen; AGM, aorta, gonad, and mesonephros; CSF-1, colony stimulating factor-1; E, embryonic age; EGA, estimated gestational age; eYFP, enhanced yellow fluorescent protein; Flt3, fms-like tyrosine kinase 3; Flt3L, Flt3 ligand; LC, Langerhans cell; Runx1, runt-related transcription factor 1; YS, yolk sac.

Epidermal Langerhans cells (LCs) belong to the DC family; a small group of tissue hematopoietic cells that specialize in the induction of adaptive immune responses. Similar to most DCs, LCs are well equipped to capture, process, and present peptide-bound MHC complexes on the cell surface and migrate from the epidermis to the skin-draining lymph nodes to present cutaneous antigens to T lymphocytes (Merad et al., 2008; Romani et al., 2010).

LCs exhibit specific differentiation and homeostatic features, which distinguish them from other DC populations. For example, whereas DC development and homeostasis are critically controlled by fms-like tyrosine kinase 3 (Flt3) ligand (Flt3L) and its receptor

Flt3 (Merad and Manz, 2009), mice lacking Flt3 or Flt3L have normal numbers of LCs in vivo (Ginhoux et al., 2009; Kingston et al., 2009). In contrast, the receptor for colony stimulating factor-1 (CSF-1R) is required for LCs to develop (Ginhoux et al., 2006), but is dispensable for the development of lymphoid tissue resident DCs (Ginhoux et al., 2009; Witmer-Pack et al., 1993). In contrast to other DCs, which are constantly replaced by a circulating pool of BM-derived committed precursors, LCs maintain themselves in situ throughout life, independent of any input from the BM (Merad et al., 2002). Furthermore, LCs resist high-dose ionized radiation and remain of host origin after lethal irradiation and reconstitution with donor congenic BM (Merad et al., 2002).

The origin of the precursors that give rise to tissue DCs are beginning to be characterized (Geissmann et al., 2010). For example, the macrophage and DC precursor gives rise to monocytes and to the common DC precursor, which has lost monocyte/macrophage differential potential and gives rise exclusively to DCs. However, none of these progenitors contribute to LC homeostasis in adult mice. In contrast, adult LC homeostasis is maintained by a pool of LC precursors that take residence in the skin before birth (Romani et al., 1986; Chang-Rodriguez et al., 2005; Chorro et al., 2009). However, the origin and the developmental regulation of these embryonic LC precursors remain unknown.

Two major hematopoietic sites contribute to blood cell formation during embryogenesis (Tavian and Péault, 2005; Orkin and Zon, 2008). In mice, the first hematopoietic progenitor appears in the extra-embryonic yolk sac (YS) shortly after the onset of gastrulation, around embryonic age (E) 7.0, leading to the initiation of primitive hematopoiesis, which consists mainly of erythrocytes and macrophages (Moore and Metcalf, 1970; Bertrand et al., 2005). Primitive macrophages spread into the embryo with the onset of blood circulation around E9.0 (Lichanska and Hume, 2000). After E8.5, with the determination of the intraembryonic mesoderm toward the hematopoietic lineage, a new wave of hematopoietic progenitors is generated within the embryo proper, first in the paraaortic splanchnopleura region, and then in the aorta, gonads, and mesonephros (AGM) region (Medvinsky et al., 1993; Godin et al., 1993). The hematopoietic stem cells generated within the AGM will lead to the establishment of definitive hematopoiesis (Orkin and Zon, 2008). Around E10.5, YS- and AGM-derived hematopoietic progenitors colonize the fetal liver (Kumaravelu et al., 2002), which serves as a major hematopoietic organ after E11.5, generating all hematopoietic lineages, including monocytes (Naito et al., 1990).

We recently showed that microglia, the resident macrophage population of the central nervous system, arise exclusively from YS-derived primitive myeloid progenitors that appear before E8.0 (Ginhoux et al., 2010). Interestingly, similar to LCs, microglial cells are also dependent on the

CSF-1R for their development (Ginhoux et al., 2010), and they resist high-dose ionized radiation and maintain themselves in situ, independent of any input from BM precursors (Ajami et al., 2007; Mildner et al., 2007). These shared cytokine requirements and homeostatic properties may suggest a common developmental origin of these two cell types. In this study, we examined the contribution of embryonic myeloid precursors to LC homeostasis in adult mice. Using in vivo lineage-tracing studies and in utero adoptive transfer strategies, we show that adult LCs derive exclusively from embryonic precursors of both YS-derived primitive macrophage and fetal liver–derived monocyte origin.

RESULTS

LC precursors are recruited to the skin before birth

Adult LCs derive from hematopoietic precursors that take residence in the skin before birth, and before the onset of BM hematopoiesis. Early studies revealed that myeloid-like cells expressing the myeloid markers F4/80 and CD11b were present in the skin during the later stages of embryonic development (Ginhoux and Merad, 2010). These cells were considered LC precursors because they were proliferating actively (Chang-Rodriguez et al., 2005; Chorro et al., 2009) and lacked mature LC markers such as MHC class II and langerin, which were acquired after birth (Romani et al., 1986; Tripp et al., 2004).

However, these studies were mainly correlative, and the potential contribution of postnatal hematopoietic progenitors to the adult LC pool in the steady state was never formally addressed. To exclude the possibility that a wave of perinatal circulating hematopoietic precursors, such as monocytes, contributes to adult LC homeostasis, we reconstituted C57BL/6 CD45.2$^+$ newborns that were sublethally irradiated in the first 24 h after birth with adult BM hematopoietic cells isolated from CD45.1$^+$ congenic mice. Donor CD45.1$^+$ cell engraftment was measured in the blood 3 mo after transplantation and showed that >30% of blood circulating leukocytes, including B and T lymphocytes, monocytes, and macrophages from lymphoid and nonlymphoid tissues, were of donor origin (Fig. 1, A and B). In contrast, >95% of LCs were of host origin at this time point (Fig. 1, A and B). Similar results were obtained after reconstitution with E14.5 fetal liver cells (unpublished data). LC chimerism was also monitored at later time points, and LCs remained of host origin for >7 mo after reconstitution (Fig. 1 B). Similar results were obtained when microglia were analyzed (Fig. 1 B), as previously reported (Ginhoux et al., 2010). Thus, similar to microglia, these results suggest that LCs are maintained independent of circulating monocytes and instead rely on local radioresistant precursors that colonize the epidermis before birth.

Primitive myeloid precursors are present in the skin rudiment of E12.5 embryos

Microglia and LCs share similar cytokine requirements and homeostatic properties that could potentially reflect

a common developmental regulation. We recently showed that adult microglia develop almost entirely from YS-derived myeloid progenitors that arise before E8.0 (Ginhoux et al., 2010). To examine the contribution of these progenitors to LCs, we first used $Cx3cr1^{gfp/+}$ and $Csf1r^{gfp/+}$ knock-in myeloid reporter mice, as CSF-1R is a key regulator of LC development (Burnett et al., 2004; Ginhoux et al., 2006) and CX3CR1 is highly expressed on myeloid precursors including embryonic microglial precursors (Jung et al., 2000; Ginhoux et al., 2006). We found that hematopoietic cells with a similar phenotype and morphology to YS macrophages were present in the developing skin of E12.5 $Cx3cr1^{gfp/+}$ embryos. We analyzed limb buds for time points before E16.5, as they are representative of embryonic skin and less subject to contamination with deeper tissues than the skin covering the embryonic body. Limb bud–infiltrating cells expressed CD11b, F4/80, CSF-1R, and high levels of CX3CR1, but lacked Gr-1 (Fig. 2, A and B). Limb bud CD11b$^+$F4/80$^+$CSF-1R$^+$ cells presented a macrophage-like morphology (intracytoplasmic vacuoles, as well as veils and ruffles on the surface), as assessed by light and scanning electronic microscopy (Fig. 2 C), were highly proliferative (Fig. 2 D) and likely correspond to the previously described YS-derived primitive macrophages that seed the embryonic tissues (Takahashi et al., 1989; Lichanska et al., 1999; Rae et al., 2007). Immunofluorescence and two-photon imaging analysis of the developing skin of E12.5 $Cx3cr1^{gfp/+}$ or $Csf1r^{gfp/+}$ embryos revealed that primitive macrophages are already outside the blood vessels and constitute a dense cellular network in the subectodermal mesenchyme, but are not yet present in the ectoderm (Fig. 2, E and F, and Video 1). Similar data were obtained at E10.5 (unpublished data). Finally, in agreement with their YS origin, these skin-infiltrating myeloid cells were absent in CSF-1R–deficient E12.5 embryos (Fig. 2, G and 2H), which lack YS macrophages (Ginhoux et al., 2010).

Fate–mapping study reveals that YS-derived primitive macrophages are the major precursors of skin-infiltrating myeloid cells in E13.5 embryos

To examine the direct contribution of YS-derived macrophages to these skin-infiltrating myeloid cells, we lineage traced YS progenitors using mice expressing tamoxifen-activated *MER-Cre-MER* recombinase gene under the control of one of the endogenous promoters of the runt-related transcription factor 1 (Runx1) locus, as previously described (Samokhvalov et al., 2007). Runx1 is expressed by hematopoietic progenitors in the extra-embryonic YS from E6.5 to E7.0 (North et al., 1999; Samokhvalov et al., 2007). We crossed the *Runx1-MER-Cre-MER* mice ($Runx1^{Cre/wt}$) with the Cre-reporter mouse strain $Rosa26^{R26R-eYFP/R26R-eYFP}$ and induced recombination in embryos by a single injection of 4-hydroxytamoxifen (4'OHT) into pregnant females. Active recombination in these knock-in mice occurs in a small timeframe that does not exceed 24 h after injection and leads to irreversible expression of the *enhanced yellow fluorescent protein* (*eYFP*) reporter gene in Runx1$^+$ cells and their progeny (Samokhvalov et al., 2007). We injected 4'OHT into pregnant $Runx1^{Cre/wt}$ females at E7.25–E7.5 and analyzed the percentage of eYFP-labeled myeloid cells in embryos when they reached E10.5 and E13.5 (Fig. 3, A–C). E10.5 embryos treated with 4'OHT at E7.25–E7.5 exhibited a strong and highly correlated proportion of labeled macrophages in the YS, limb buds, and brain rudiment (Fig. 3, A and B). Furthermore, the proportion of eYFP$^+$ cells within these three populations was similar in E10.5 and E13.5 embryos treated with 4'OHT at E7.25–E7.5 (Fig. 3, B and C). The partial labeling of Runx1$^+$ YS cells is inherent to in vivo labeling techniques and likely results from the insufficient expression of *MER-Cre-MER* and limited availability of the ligand in target cells (Samokhvalov et al., 2007). Thus, our model likely underestimates the contribution of Runx1$^+$ precursors to fetal macrophages, although we cannot exclude the potential contribution of nonlabeled precursors to this process.
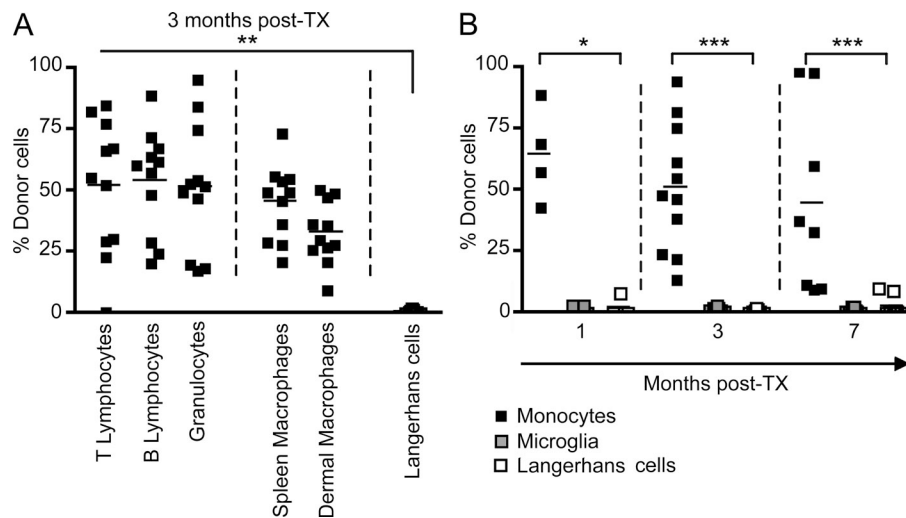

Figure 1. Adult LCs arise from embryonic precursors. Newborn CD45.2$^+$ mice were reconstituted with bone marrow cells isolated from adult CD45.1$^+$ mice. (A) Percentage donor-derived cell populations 3 mo after newborn transplantation (TX). Each data point represents a single mouse. Bars represent means of data from 4 pooled experiments ($n = 11$). The gating strategy for each leukocyte population was described previously (Ginhoux et al., 2010). (B) Percentage donor-derived monocytes, microglial cells, and LCs at different time points after reconstitution. Bars represent means of data from 4 pooled experiments ($n = 4–11$). ***, P < 0.0001; **, P < 0.001; *, P < 0.01.
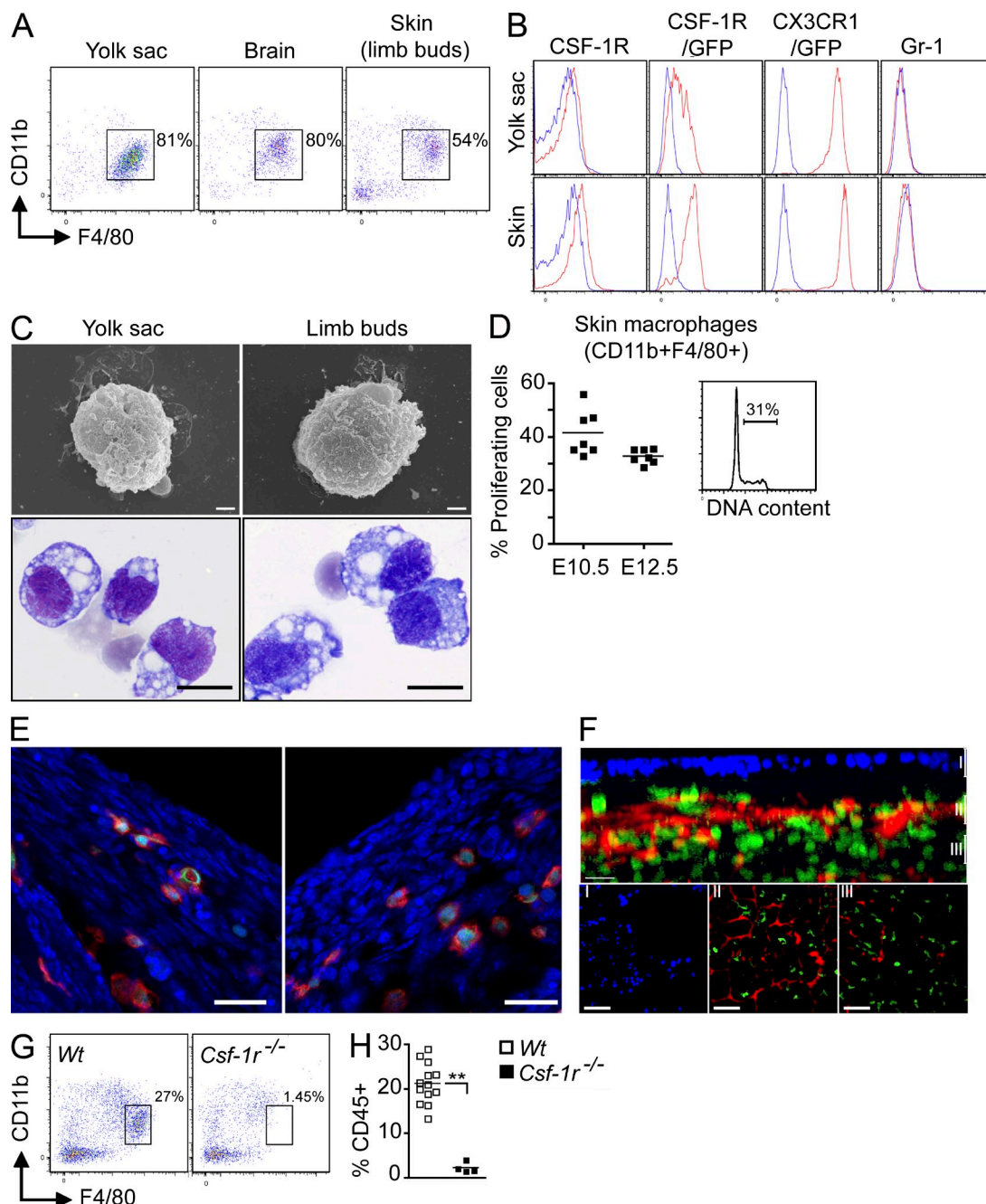
Figure 2. Fetal macrophages are already present in the skin rudiment of E12.5 embryos. (A and B) CD11b and F4/80 expression on gated DAPI⁻CD45⁺ cells isolated from indicated tissues of E12.5 embryos. (B) Expression of indicated cell surface markers or GFP reporters (red) compared with isotype/WT controls (blue) on DAPI⁻CD45⁺CD11b⁺F4/80⁺ cells from YS or skin (limb buds) isolated from WT, *Cx3cr1^gfp/+*, and *Csf1r^gfp/+* embryos. Data are representative of 3 independent experiments (*n* = 6 mice). (C) E12.5 YS or limb bud macrophages were sorted based on their phenotype (DAPI⁻CD45⁺CD11b⁺F4/80⁺) and harvested onto cytospin slides for SEM microscopy (top; bar, 1 µm) or Wright-Giemsa staining (bottom; bar, 5 µm). Data are representative of two independent experiments. (D) Flow cytometric cell cycle analysis of CD45⁺F4/80⁺CD11b⁺ macrophages present in E10.5 and E12.5 limb buds. Data from two pooled experiments (*n* = 6 to 7). (E) Cross sections of developing skin obtained from E12.5 *Cx3cr1^gfp/+* embryos were labeled with anti-F4/80 monoclonal antibody (red) and counterstained with DAPI that label nuclei (blue). Data are representative of 2 experiments (*n* = 2; bar, 30 µm). (F) High magnification image of CSF-1R^gfp cells (green) in *Csf1r^gfp/+* E12.5 developing skin acquired by two photon microscopy. Evans blue stains the blood vessels (red) and DAPI (blue) stains the superficial layer of the epidermis. Top panel illustrates the side view of these 3D reconstructions, and top view snapshots at different depths are shown in the bottom panels (Bars: I, ∼30 µm; II, ∼60 µm; III, ∼90 µm). Bars: 80 µm (top); 30 µm (side). Data are representative of 2 experiments (*n* = 2). (G and H) CD11b and F4/80 expression on gated DAPI⁻CD45⁺ cells isolated from E12.5 *Csf-1r^−/−* or control littermate (*Wt*) FVB/NJ embryos. (H) Percentage fetal macrophages (F4/80⁺CD11b⁺) isolated from E12.5 *Csf-1r^−/−* or control littermate (*Wt*) mice. Pooled data from three separate experiments. **, P < 0.001.
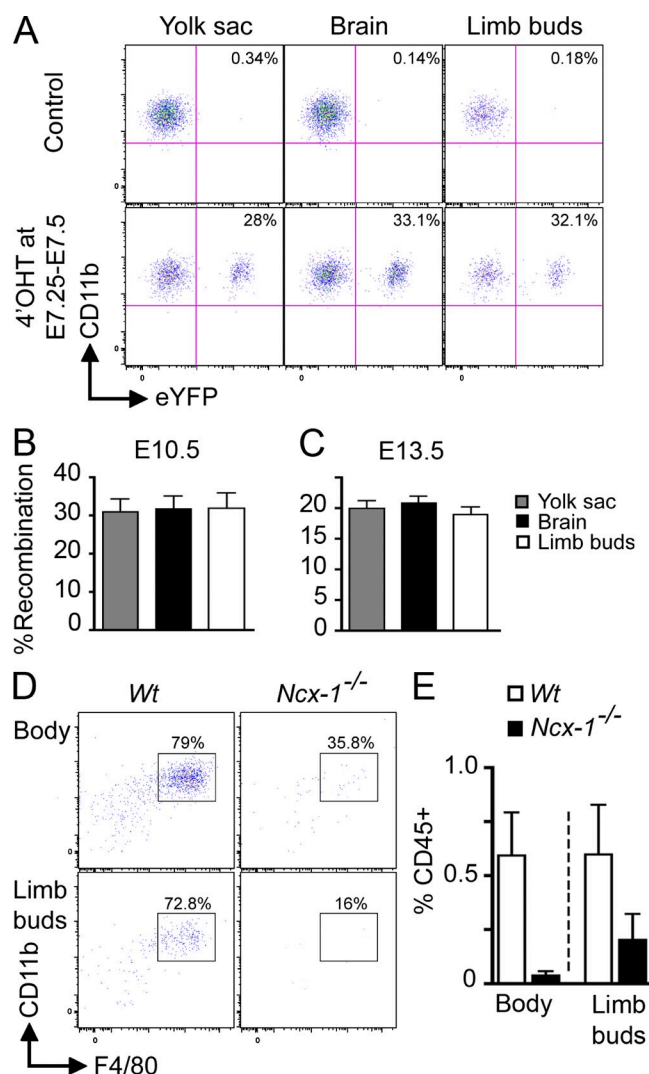
Figure 3. YS–derived primitive macrophages are the major precursors of skin–infiltrating macrophages in E10.5 and E13.5 embryos. (A–C) *Runx1^{Cre/wt} : Rosa26^{R26R-eYFP}* embryos were treated with 4'OHT to induce Cre-mediated recombination at E7.25–E7.5 followed by analysis at E10.5 (A and B) or E13.5 (C). Controls are nontreated mice. (A) Flow cytometric analysis from one representative control or treated E10.5 embryo, showing the percentage recombination (eYFP+ cells) within CD45+CD11b+F4/80+ cells isolated from YS, brain rudiment, and limb buds at E10.5. (B and C) Percentage recombination within CD45+CD11b+F4/80+ cells isolated from the indicated tissues at E10.5 and E13.5. Error bars represent mean ± SEM of pooled data from 2 experiments (n = 8–16). (D and E) Developing skin (body and limb buds) was isolated from E10.0–E10.5 Ncx1^{−/−} embryos or control littermates and processed for flow cytometric analysis. (E) Percentage ± SEM of hematopoietic cells (CD45+) in control littermates (white bars, n = 4) and Ncx1^{−/−} embryos (black bars, n = 3). Pooled data from two independent experiments.

YS–derived primitive macrophages migrate through blood circulation to infiltrate embryonic skin

To visualize the recruitment of primitive macrophages to the skin during early development, we injected *Runx1^{Cre/wt}: Rosa26^{R26R-LacZ}* embryos with a single dose of 4'OHT at E7.25–E7.5 and traced the appearance of Runx1+ precursor progeny into the skin of E10.0 embryos. A large number of Lac-Z+ cells appeared to be associated with blood vessels and infiltrated the skin rudiment in E10.0 conceptus (unpublished data). To address whether the development of functional blood vessels was required for the recruitment of primitive macrophages to the skin rudiment, we used *Ncx-1^{−/−}* animals that lack a heartbeat and functional blood circulation because of a defect in the sodium calcium exchanger 1 (Koushik et al., 2001). We found that E10.0–E10.5 *Ncx-1^{−/−}* embryos have WT levels of YS macrophages (Ginhoux et al., 2010), but no skin–infiltrating macrophages, whereas *Ncx-1^{+/+}* control littermates already have a substantial number of macrophages in the skin rudiment at this time point (Fig. 3, D and E). Altogether, these results suggest that CSF-1R–dependent Runx1+ YS primitive macrophages migrate from the YS through blood vessels to seed the developing skin in the subectodermal mesenchyme, as early as E10.0.

YS–derived primitive macrophages contribute to adult LCs

The aforementioned results establish that YS-derived primitive macrophages infiltrate the embryonic skin before the full development of fetal liver hematopoiesis. To examine whether YS-derived macrophages contribute to the maintenance of LCs in the normal steady state adult skin, we injected 4'OHT into pregnant *Runx1^{Cre/wt}* females at E7.25–E7.5, as previously described, and analyzed and treated the embryos when they reached 6–8 wk of age. In adult mice treated with 4'OHT at E7.25–E7.5, ∼6% of LCs were eYFP+ (Fig. 4, A and B). In contrast, 2% of blood leukocytes (circulating monocytes, T cells, B cells, and granulocytes) and tissue macrophage (such as lung macrophages) were eYFP+ in these mice. The low level of tagging expressed by all leukocytes reflects the previously reported contribution of YS progenitors to adult hematopoietic stem cells (Samokhvalov et al., 2007). We also examined the earliest stage at which Runx1+ progenitors contributed to the adult LC pool. In adult mice treated with 4'OHT between E7.0–E7.75, 2–3% LCs were eYFP+, whereas no more than 0.2% circulating monocytes were eYFP+ (Fig. 4 C). These results establish that primitive myeloid progenitors that arise before E7.5 contribute significantly more to the adult LC pool than other leukocytes.

A second wave of LC precursors colonizes the developing skin during late embryogenesis

Fate-mapping studies of Runx1+ precursors revealed that the majority of skin-infiltrating myeloid cells in E13.5 embryos derive from YS primitive macrophages, as indicated by the levels of recombination, which reached 20% and were identical in the YS and skin-infiltrating macrophages (Fig. 3 C). However, the percentage of eYFP+ cells among LCs did not exceed 6–7% in adult mice (Fig. 4 B). Because adult LCs derive from precursors that are recruited to the skin before birth (Fig. 1), we hypothesized that a second wave of progenitors
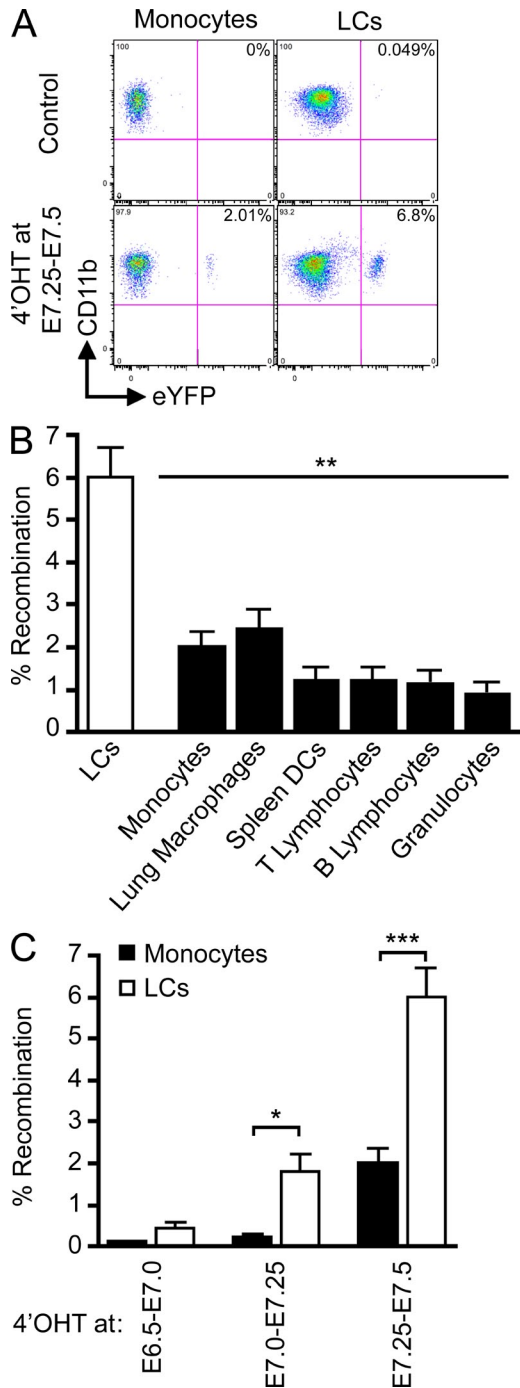
Figure 4. Primitive YS–derived macrophages contribute to adult LCs.
Runx1^Cre/wt : *Rosa26*^R26R-eYFP embryos were treated with 4'OHT to induce Cre-
mediated recombination at different time-points of development and analyzed
during adulthood at 8–10 wk post-birth. Controls are nontreated mice. (A) Flow
cytometric analysis from one representative control adult or 4'OHT-treated adult
(treated at E7.25-E7.5), showing the % recombination (eYFP+ cells) within blood
monocytes and epidermal LCs. (B) Pooled data from 3 experiments showing the
% recombination among epidermal LCs and various indicated cell population
from mice treated with 4'OHT at E7.25-E7.5. (C) Percentage recombination within
monocytes (black bars) and epidermal LCs (white bars) in adult mice treated with
4'OHT at the indicated embryonic ages. Error bars represent mean ± SEM of
pooled data from 2 experiments (*n* = 8). ***, P < 0.0001, **, P < 0.001; *, P < 0.01.

independent of YS macrophages infiltrated the skin after
E13.5 and likely contributed to the dilution of the eYFP
signal in the adult LC compartment.

Using flow cytometry, we first analyzed the myeloid
cell content of the developing epidermis at E16.5–E17.5,
the earliest time point when separate analysis of the epider-
mal and dermal compartment can be easily performed. We
found that E17.5 epidermal-infiltrating myeloid cells ex-
pressed the monocyte/macrophage markers CD11b, F4/80,
CSF-1R, and CX3CR1, and that they lacked Gr-1 (Fig. 5 A).
These cells also presented a macrophage-like morphology
(Fig. 5 B), were highly proliferative (Fig. 5 C), and acquired
adult LC markers (langerin and MHC class II molecules)
within the week after birth (not depicted), as previously
reported (Chang-Rodriguez et al., 2005; Chorro et al.,
2009). The remaining CD45+CD11b−F4/80− cells expressed
T cells markers (Thy, CD3, and Vγ3) and correspond to
dendritic epidermal T cell progenitors (unpublished data).
Imaging of *Cx3cr1*^gfp/+ or *Csf1r*^gfp/+ embryos revealed that
GFP+F4/80+ cells start to appear in the epidermis around
E16.5 (Fig. 5, D and E), although rare cells were sometimes
detected at E15.5 (Video 2). Epidermal GFP+ cells present
in the epidermis just below the skin surface (highlighted by
the DAPI+ layer), exhibited a more dendritic morphology
than dermal GFP+ cells (Fig. 5 E and Videos 2, Video 3, and
Video 4). Finally, consistent with previous data showing
that adult LCs are absent in CSF-1R–deficient mice (Ginhoux
et al., 2006), epidermal-infiltrating myeloid cells were ab-
sent from the epidermis of CSF-1R–deficient E17.5 em-
bryos (Fig. 5, F and G).

Using the aforementioned fate-mapping system, we
found that the percentage of eYFP+ cells among epidermal-
infiltrating myeloid cells decreases to adult levels around
E16.5 (Fig. 6 A). These results suggest that E7.5 Runx1+ YS
progenitor cells are the main precursors of skin-infiltrating
myeloid cells until at least E13.5, but that other precursors
were recruited to the developing skin between E13.5 and
E16.5 and contributed to the dilution of the eYFP signal
observed in adult LCs of 4'OHT-treated embryos. To trace
when during development the second wave of myeloid pre-
cursors appears in the embryo, we injected 4'OHT at later
time points (E7.5–E7.75, E8.5, and E9.5). The proportion of
eYFP+ LCs in adult mice was significantly higher in mice
treated with 4'OHT at E8.5 and E9.5 compared with mice
treated with 4'OHT at E7.25–E7.5 (25–30% versus 6%, re-
spectively) and was identical to the percentage eYFP+ leuko-
cytes thought to derive from definitive hematopoiesis, such
as monocytes (Fig. 6 B). Together, these results suggest that
adult LCs derive from two distinct waves of myeloid progen-
itors: one that arises in the YS at E7.5 and is recruited to the
skin around E10.5 and defined as the primitive wave (Palis
et al., 1999), and another that is recruited to the developing
skin between E13.5 and E16.5 and arises at E8.5–E9.5 (either
in the YS during a second wave of hematopoiesis [Palis et al.,
1999; Bertrand et al., 2005] or in the paraaortic/splanchnopleura
and AGM region).
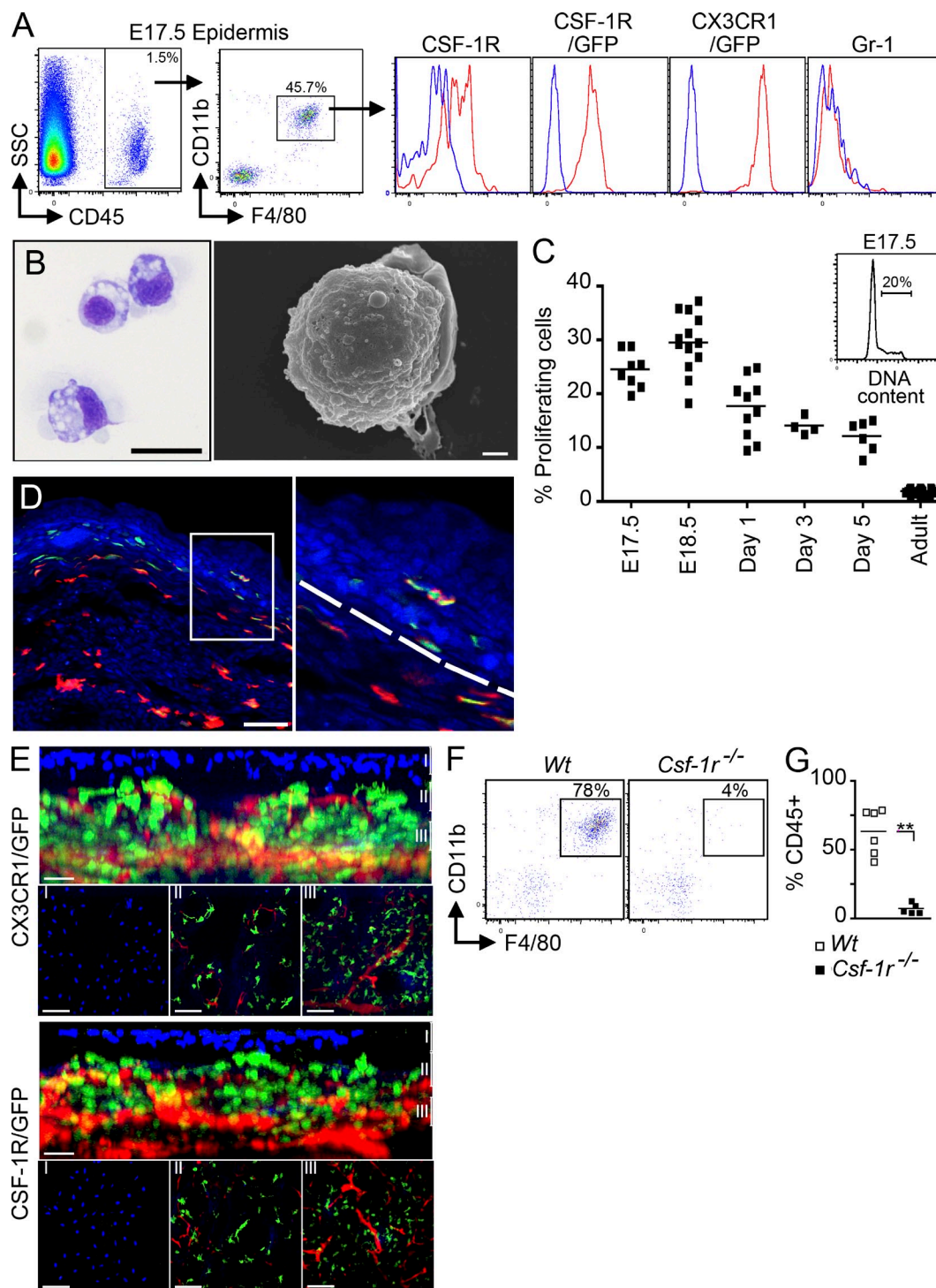
Figure 5. Characterization of LC precursors in embryonic early epidermis. (A) Flow cytometric analysis of gated DAPI⁻CD45⁺ cells from E17.5 epidermis. Histograms show expression of cell surface markers or GFP reporters (red) compared with isotype/WT controls (blue) on gated DAPI⁻CD45⁺CD11b⁺F4/80⁺ cells. Data are representative of 3 independent experiments (*n* = 6 mice). (B) Cytospin and SEM of sorted E17.5 myeloid cells (as in Fig. 2 C). Data are representative of two independent experiments. (C) Flow cytometric cell cycle analysis of CD45⁺F4/80⁺CD11b⁺ LC precursors at different stages of embryonic development or early postnatal development and adult LCs. Data from 2 pooled experiments (*n* = 4–13 mice). (D) Skin cross sections obtained from E16.5 *Cx3cr1^gfp/+* embryos were labeled with anti-F4/80 monoclonal antibody (red) and counterstained with DAPI that label nuclei (blue). Higher magnification image reveals the presence of F4/80⁺CX3CR1/GFP⁺ LC precursors in the epidermis at E16.5 (bar, 50 µm). Data are representative of 2 independent experiments (*n* = 4). (E) Three-dimensional reconstructions of image stacks taken by multiphoton microscopy from E16.5 developing skin of *Cx3cr1^gfp/+* or *Csf1r^gfp/+* embryos. DAPI (blue) stains the superficial layer of the epidermis, and blood vessels are highlighted in red using Evans blue (as in Fig. 2 F; data are representative of 2 experiments, *n* = 2). Bars: 80 µm (top); 30 µm (side). (F and G) Percentage LC precursors (F4/80⁺CD11b⁺) among DAPI⁻CD45⁺ circulating leukocytes isolated from E17.5 *Csf-1r^−/−* or control littermate (*Wt*) FVB/NJ embryos. Pooled data from three separate experiments.
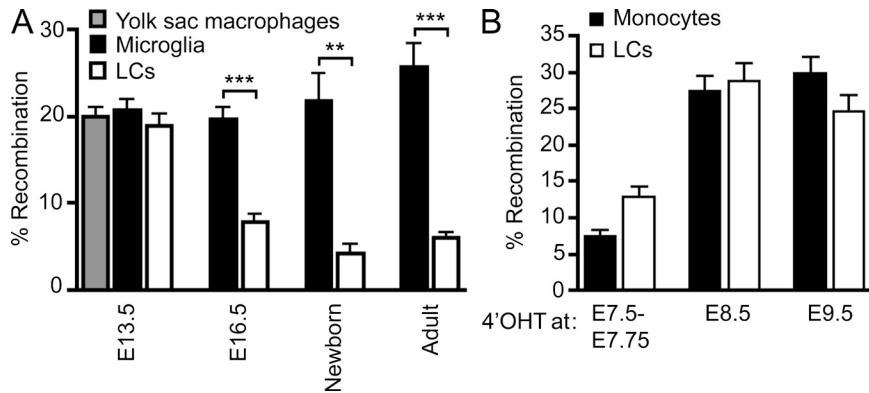
Figure 6. YS macrophage–derived LC precursors are partly replaced during late embryogenesis. (A) Percentage recombination among E13.5 YS macrophages (CD45$^+$CD11b$^+$F4/80$^+$Gr-1$^-$; gray bar); E13.5 and E16.5 microglial progenitors (CD45$^+$CD11b$^+$F4/80$^+$Gr-1$^-$) and adult microglia (CD45^{lo}CD11b$^+$F4/80$^+$Gr-1$^-$; black bars); and limb buds YS macrophages (E13.5), epidermal LC precursors (E16.5, newborn), and adult LCs (white bars) from *Runx1$^{Cre/wt}$*:Rosa26$^{R26R-eYFP}$ embryos treated with 4'OHT at E7.25–E7.5. Error bars represent mean ± SEM of pooled data from 2 experiments (n = 6–15). **, P < 0.01; ***, P < 0.0001. (B) Percentage recombination within monocytes and epidermal LCs in adult mice treated with 4'OHT at the indicated embryonic ages. Error bars represent mean ± SEM of pooled data from 2 experiments (n = 3–15 mice).

Fetal liver–derived monocytes differentiate into LC precursors in the developing skin

Our results suggest that a second wave of Runx1$^+$ myeloid progenitors arises at E8.5 and is recruited to the skin between E13.5 and E16.5. Prior results have suggested that a definitive wave of granulocyte/macrophage progenitors (in opposition to the first YS primitive wave) arises either in the YS or in the embryo proper before migrating to the fetal liver (Palis et al., 1999), where they undergo further maturation followed by differentiation into mature hematopoietic cells from E11.5.

We have previously found that adult monocytes can differentiate in vivo into LC precursors in adult murine inflamed skin (Ginhoux et al., 2006), and therefore hypothesized that fetal liver monocytes could potentially give rise to LCs during embryonic life. Fetal liver monocytes, defined as CD45$^+$CD11b$^+$F4/80$^+$CSF-1R$^+$CX3CR1$^{+/-}$Gr-1$^{+/-}$ cells are a product of fetal liver hematopoiesis and pro-monocytes can be detected in the fetal liver around E12.5 (Naito et al., 1990). Using flow cytometry, we found that CD11b$^+$F4/80$^+$Gr-1$^+$ monocyte-like cells are recruited to the developing skin from E14.5 onward (Fig. 7 A). Circulating fetal liver–derived monocytes (CD11b$^+$F4/80$^+$CSF-1R$^+$CX3CR1$^{+/-}$Gr-1$^{+/-}$) are found just before in the blood from E13.5–E14.5 (Fig. 7 B, bottom).

Thus, the E16.5 prospective dermis contains two phenotypically distinct populations that differentially expressed CD11b and F480 among CD45$^+$ cells (Fig. 7 B, top). The CD11b^{hi}F480^{lo}CX3CR1^{int} population (population *P1*) likely corresponds to fetal liver–derived monocytes recruited to the developing skin, as they resemble phenotypically the fetal liver and blood circulating monocytes (Fig. 7 B). Both populations express similar levels of CD11b, F4/80, CXCR1 and included similar proportions of Gr-1$^+$ and Gr-1$^-$ cells. They also presented a similar morphology as shown by cytospin and SEM imaging (Fig. 7 D). In contrast, the CD11b^{lo}F480^{hi}CX3CR1^{hi} population (population *P2*) expresses high CX3CR1 and F4/80 levels and lack Gr-1 and resemble phenotypically YS macrophages (Fig. 2, A and B), as well as LC precursors found in E17.5 embryos (Fig. 5 A). They also presented a similar macrophage-like morphology (Fig. 2 C, Fig. 5 B, and Fig. 7 D). Finally, similarly to Runx1$^+$ YS macrophages

(Fig. 2 G) and epidermal LC precursors (Fig. 5 F) that are strictly dependent on CSF-1R for their development, the *P2* population was completely missing in the skin of E15.5 CSF-1R–deficient mice (Fig. 7 C). In contrast, absence of CSF-1R did not affect monocyte development in the fetal liver and their recruitment to the skin, as P1 cells were unaffected in E15.5 skin of CSF-1R–deficient mice (Fig. 7 C).

We also analyzed the proportion of eYFP$^+$ cells among populations *P1* and *P2* in E16.5 embryos treated with 4'OHT at E7.5 (to label the contribution of the primitive wave) or E8.5 (to label the contribution of the nonprimitive wave). Similar to fetal liver monocytes and adult blood monocytes, population *P1* was not labeled in 16.5 embryos treated with 4'OHT at E7.5, but reached >30% eYFP$^+$ cells in embryos treated with 4'OHT at E8.5 (Fig. 7 E). In contrast, the proportion of eYFP$^+$ cells among population *P2* was similar to that of adult LCs and reached 6% eYFP$^+$ cells in embryos treated with 4'OHT at E7.5 and 30% eYFP$^+$ cells in embryos treated with 4'OHT at E8.5 (Fig. 7 E).

Based on these results, we hypothesized that fetal liver–derived monocytes are recruited to the prospective dermis from E13.5 to E16.5 (population *P1*), where they differentiate into LC precursors (population *P2*) in a CSF-1R–dependent manner, before their recruitment to the epidermis around E16.5. To definitely determine whether fetal liver monocytes can give rise to LC precursors in the fetal skin, we adoptively transferred fetal liver monocytes isolated from E13.5–E14.5 congenic C57BL/6 *Cx3cr1$^{gfp/+}$* CD45.1$^+$ embryos into E13.5–E14.5 C57BL/6 CD45.2$^+$ host embryos in utero (2–3.10^5 monocytes per embryo; Fig. 8 A). Donor-derived monocytes were detected in the blood (Fig. 8, B and D) and in the skin (Fig. 8, C and D) of recipient embryos as early as 3 h after adoptive transfer, but were always absent from the brain (not depicted). Engraftment variability observed in recipient mice was embryo dependent and not experiment dependent (unpublished data). Analysis at later time points after transfer (48 and 72 h corresponding to E16.5 and E17.5, respectively) revealed that adoptively transferred fetal liver monocytes (population *P1*) give rise to transitional cells, that down-regulated
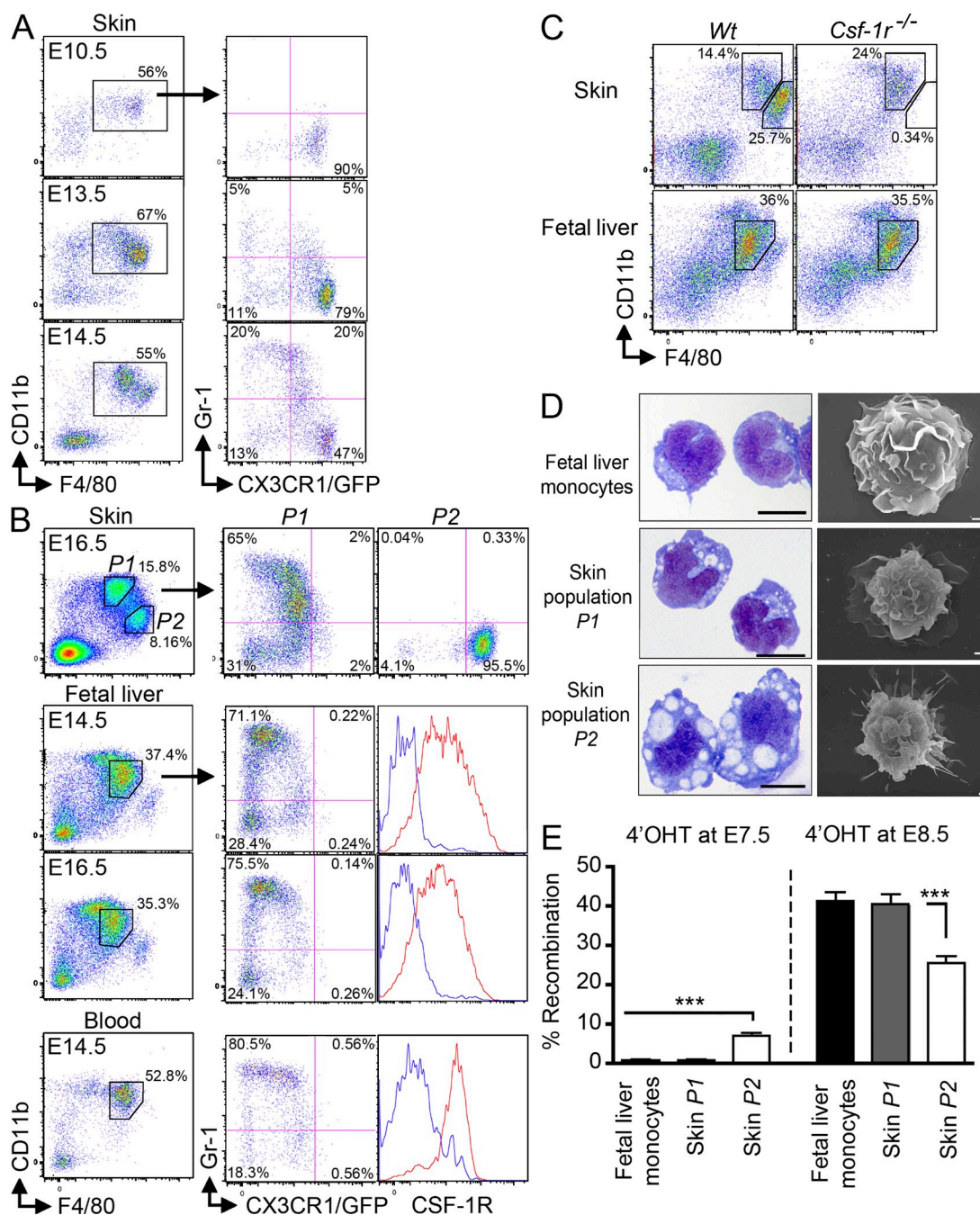
Figure 7. Fetal liver monocytes are recruited to the developing skin from E14.5. (A and B) Expression of Gr-1 and CX3CR1^{gfp} in gated DAPI$^-$CD45$^+$CD11b$^+$F4/80$^+$ cells isolated from the indicated tissues of *Cx3cr1$^{gfp/+}$* embryos at the indicated stage of development. (B) Histograms show expression of CSF-1R (red) compared with isotype control (blue) on gated cells. Data are representative of 3 independent experiments (*n* = 3). (C) Expression of CD11b and F4/80 on gated DAPI$^-$CD45$^+$ cells isolated from the skin or fetal liver of E15.5 *Csf-1r$^{-/-}$* or control littermate (*Wt*) FVB/NJ mice. Data are representative of 2 independent experiments (*n* = 3). (D) Indicated populations were sorted from E16.5 *Cx3cr1$^{gfp/+}$* embryos based from on their described phenotype and harvested onto cytospin slides for Wright-Giemsa staining (left; bar, 5 µm) or SEM microscopy (right; bar, 1 µm). Data are representative of two independent experiments. (E) Percentage recombination within the indicated gated populations isolated from E16.5 fetal liver or prospective dermis from *Runx1$^{Cre/wt}$* : Rosa26$^{R26R-eYFP}$ embryos treated with 4'OHT at E7.25–E7.5 or E8.5. Error bars represent mean ± SEM of pooled data from 2 experiments (*n* = 6–12). ***, P < 0.0001.

Gr-1 and up-regulated CX3CR1 before differentiating into LC precursors (population *P2*; Fig. 8, E and F). By E19.5 (5 d after transfer), all donor monocytes had differentiated

into *P2*-like cells (Fig. 8, E [bottom] and F). Noninjected embryos or embryos injected with Ter119$^+$ erythroid progenitors were used as negative controls (Fig. 8, D and G).
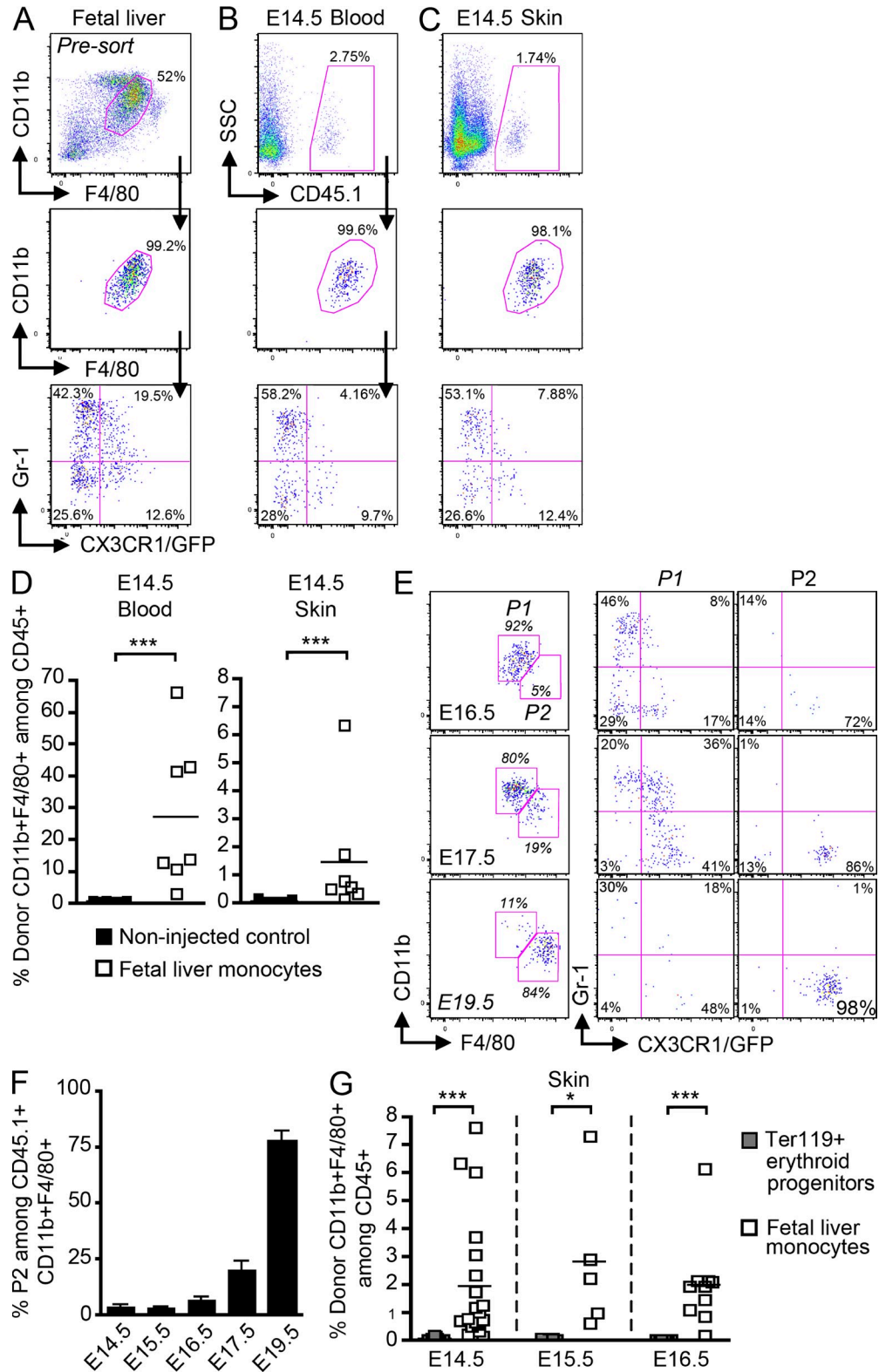
Figure 8.   Fetal liver monocytes differentiate into LC precursors. Monocytes were purified from E13.5–E14.5 fetal liver of *Cx3cr1*[gfp/+]CD45.1[+] mice and adoptively transferred in utero into unconditioned E13.5–E14.5 CD45.2[+] congenic embryos. (A–C) Flow cytometry analysis of the progeny of adoptively transferred CD45.1^{+} monocytes (A) in the blood (B) and skin (C) 3 h after injection. (A) Gating strategy (top) for monocytes among fetal liver leukocytes (DAPI^{−}CD45^{+}), purity after sorting (middle), and profile of expression for Gr-1 and CX3CR1/GFP (bottom). (B and C) Percentage CD45.1^{+} donor-derived monocytes among total CD45^{+} cells (top), expression of CD11b and F4/80 (middle), and Gr-1 and CX3CR1/GFP (bottom) among indicated

Strikingly, we also found that progeny of adoptively transferred monocytes were also detectable in E19.5 epidermis (5 d after transfer; Fig. 9, A and B), exhibiting a phenotype similar to the phenotype of endogenous LC precursors (Gr-1⁻CX3CR1ʰⁱ) found in E16.5 prospective dermis (Fig. 7 B) and in E17.5 epidermis (Fig. 5 A). Importantly, donor monocytes-derived LC precursors up-regulated MHC II at day 2 after birth (Fig. 9 C), suggesting that they differentiated into epidermal LCs as observed for endogenous LC precursors (Chang-Rodriguez et al., 2005).

Adult blood monocytes are composed of two major subsets, namely the Gr-1ʰⁱCX3CR1ˡᵒ and Gr-1ˡᵒCX3CR1ʰⁱ subsets (Geissmann et al., 2010). Gr-1ʰⁱ and Gr-1ˡᵒ monocyte subsets were also found in E14.5 fetal liver and blood (Fig. 7 B), although expression of CX3CR1 was more heterogeneous compared with adult monocytes (Geissmann et al., 2010). To assess the LC potential of these two subsets, we adoptively transferred purified Gr-1ʰⁱ and Gr-1ˡᵒ fetal liver monocyte subsets in utero into E14.5 embryos. Our results show that Gr-1ʰⁱ and Gr-1ˡᵒ monocytes were both able to differentiate into LC precursors in E18.5 epidermis (Fig. 9 D). In addition, LC potential was not restricted to embryonic fetal liver monocytes, as adoptively transferred adult bone marrow monocytes (purified as Gr-1⁺CD11b⁺F4/80⁺ cells) into E14.5 embryos also differentiated into epidermal LC precursors in E17.5 prospective epidermis (unpublished data).

Collectively, these results show that fetal liver monocytes infiltrate the prospective dermis during late embryogenesis and differentiate into LC precursors in a CSF-1R–dependent manner; these precursors are subsequently recruited to the epidermis to give rise to epidermal LCs during the early postnatal period.

DISCUSSION

Using fate-mapping and adoptive transfer strategies, we found that LCs that populate the normal noninflamed adult skin have a dual origin and derive from YS primitive macrophages that arise before E7.5 and fetal liver monocytes that arise from post-E7.5 myeloid progenitors. Based on early labeling that allows us to follow the YS progeny alone (E7.0–E7.5), the contribution to the adult LC pool from YS-derived fetal macrophages is ∼10–20% as estimated by normalization of the YS progenitor contribution to LCs (2 to 7%) to their microglial contribution (25–30%), assuming that the YS progenitors are the sole contributor to microglia.

E7.5 YS–derived primitive macrophages migrate through blood vessels to the developing skin around E9.5-E10.0 to give rise to myeloid precursors, whereas post-E7.5 myeloid progenitors migrate first to the fetal liver where they differentiate into monocytes before migrate to the prospective dermis and differentiate into LC precursors around E16.5. These two waves of progenitors collaborate in shaping the LC precursors that populate the E16.5 prospective dermis, which in turn give rise to the adult LC pool. However, due to the partial tagging of our fate mapping system, we cannot formally exclude the potential contribution of additional non-Runx1+ precursors to LC homeostasis.
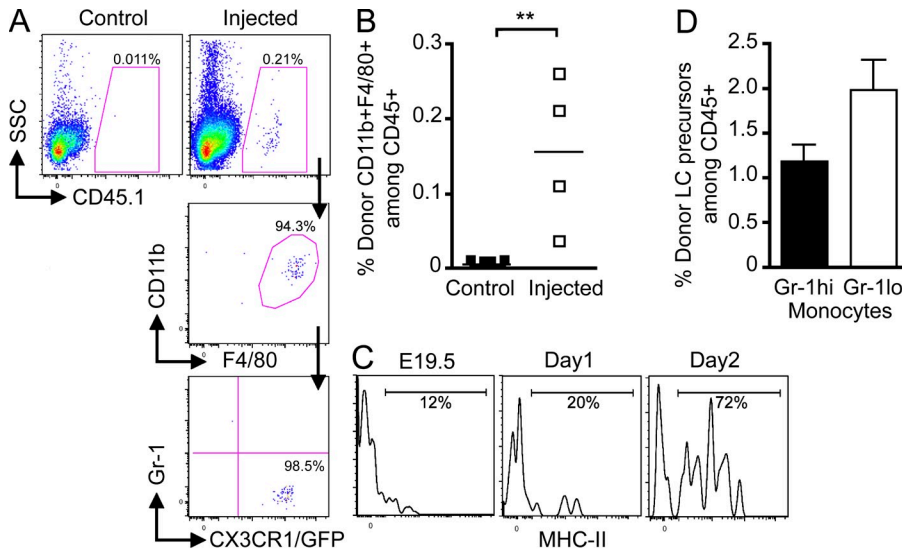
Our finding that YS-derived primitive macrophages possess LC potential is in agreement with earlier studies. Several studies have shown that LC-like cells are present in epidermal sheets derived from grafted limb buds isolated at E10.5 or E11.5, before the development of fetal liver–derived hematopoiesis (Breathnach et al., 1968; Reams and Tompkins, 1973; Silvers, 1957). Similarly in humans, LC progenitor-like cells can be found in embryos around 9 wk of estimated gestational age (EGA; Foster et al., 1986; Schuster et al., 2009). Human hematopoiesis begins in the YS around day 19 EGA, moves transitorily to the fetal liver around 4–5 wk EGA, before being definitively established in the BM (10.5 wk EGA; Tavian and Péault, 2005). Although the contribution of YS progenitors to adult human LCs remains speculative, these observations suggest that both rodent and human LCs are present in the epidermis before the onset of BM hematopoiesis.

The factors that control the recruitment of LC precursors to the embryonic epidermis remain unknown. Unlike adult inflamed skin (Bogunovic et al., 2006), where monocyte recruitment and differentiation into epidermal LCs is dependent on the secretion of CCR2 and CCR6 ligands in the skin and on the expression of CCR2 and CCR6 on LC precursors, the recruitment of LC precursors to the embryonic or fetal epidermis is independent of these receptors. CCR2 and CCR6 ligands are not expressed in fetal skin at this stage (E15.5–E17.5), and mice lacking CCR2 and CCR6 have normal numbers of epidermal LCs (Sato et al., 2000; not depicted). Interestingly, in rodents and humans, LC precursors that are present in the dermis migrate to the epidermis at a similar stage of skin development when the epidermis loses its periderm while acquiring the stratum corneum, which occurs around E16.5–E17.5 in mice and between 8 and 12 wk EGA in humans (Holbrook and Odland, 1975; Weiss and Zelickson, 1975). The periderm is a superficial cellular layer

populations. (D) Percentage cells derived from donor monocytes for each injected embryo ($n = 7$) in E14.5 blood and skin 3 h after transfer. Control represents noninjected embryos ($n = 9$). Bars show means of data from one representative experiment of three. (E) Percentage populations *P1* (CD11bʰⁱF480ˡᵒ) and *P2* (CD11bˡᵒF480ʰⁱ) on gated DAPI⁻CD11b⁺F480⁺CD45.1⁺ donor-derived cells isolated from the skin at indicated time points after transfer (E14.5) and their corresponding profile of expression for Gr-1 and CX3CR1/GFP. (F) Percentage population *P2* on gated DAPI⁻CD11b⁺F480⁺CD45.1⁺ donor derived cells isolated from the skin at indicated time points after transfer. Error bars represent mean ± SEM of pooled data from two experiments ($n = 3$ to 8). (G) Graph shows the percentage of skin CD11b⁺F4/80⁺ cells derived from donor fetal liver monocytes (white squares) or donor fetal liver Ter119⁺ erythroid progenitors (gray squares; $n = 4$–11) for each injected embryo at the indicated time points. Bars represent means of data at each time point. ***, $P < 0.0001$; *, $P < 0.01$.

derived from basal keratinocytes that provides a transitory cover for the fetal epidermis (M'Boneko and Merker, 1988). The function of the periderm is not well described, but may be related to transport/exchange between the fetus and the amniotic fluid. Another potential role for the periderm could be the regulation of the recruitment and/or differentiation of LC precursors present in the prospective dermis, before their recruitment in the epidermis.

Adult CSF-1R–deficient mice lack LCs, but the exact role of CSF-1R in LC homeostasis remains unclear. In this study, we show that LC precursors are absent in E17.5 epidermis of CSF-1R–deficient embryos, highlighting the critical role of CSF-1R signaling in the production of LC precursors of both origins. YS macrophage-derived and fetal liver–derived LC precursors are absent from the developing skin of $Csf1r^{-/-}$ embryos. Interestingly, YS-derived primitive macrophages are present, although reduced in numbers, in the YS and the subectodermal mesenchyme of E10.5 $Csf1r^{-/-}$ embryos (unpublished data). Fetal liver monocytes (Ginhoux et al., 2010) and skin-infiltrating monocytes are not affected by CSF-1R deficiency, which suggests that the production and the recruitment of YS macrophages and fetal liver monocytes to the developing skin is independent of CSF-1R, whereas their survival and/or differentiation into LC precursors is strongly dependent on CSF-1R. CSF-1 is expressed in mouse fetal and extraembryonic tissues at various stages of development, including in the amniotic fluid (Azoulay et al., 1987), and is thus a candidate factor for sustaining the differentiation and/or survival of LC progenitors. IL-34 is a recently identified alternative ligand of CSF-1R in mice and humans (Lin et al., 2008; Wei et al., 2010), but its expression has not been characterized in embryonic skin. However, in $Csf1^{op/op}$ mice, which carry a mutation in the gene encoding CSF-1 (Yoshida et al., 1990), there is a dramatic reduction in the number of LCs at birth (Dai et al., 2002), but normal numbers of adult LCs (Takahashi et al., 1992), which together suggest a critical role of IL-34 in LC differentiation after birth. Consistent with this possibility, expression of IL-34 in the skin is strongly up-regulated after birth (Wei et al., 2010; unpublished data).

The dual origin of LCs is in contrast to the singular origin of microglia, which derive mostly from YS-derived primitive myeloid progenitors (Ginhoux et al., 2010). Lack of differentiation of fetal liver–derived monocytes into microglial progenitors could result from their lack of intrinsic differentiation potential or lack of access to the developing brain. Corroborating the latter hypothesis, the blood–brain barrier is established approximately at E13.5, at the time of fetal liver monocyte release into the blood circulation (Daneman et al., 2010), but after YS-derived macrophages start to invade the neuroepithelium at E10.5 (Ginhoux et al., 2010). Adult monocytes can infiltrate the brain parenchyma and differentiate into microglial-like cells in the inflamed state, but not in the steady state, suggesting that entry of mature progenitors into the brain only occurs only through a damaged blood–brain barrier (Ajami et al., 2007; Mildner et al., 2007). In contrast, fetal liver monocytes can migrate to the prospective dermis during late embryogenesis and together with YS-derived fetal macrophages contribute to the maintenance of the LC pool throughout life in the steady-state. We speculate that YS macrophages would be the sole contributor to the adult LC pool if the access to the fetal skin would be limited as it is in the brain.

A recent study reported that YS macrophages contribute to LCs and microglia, as well as liver, pancreatic, and lung macrophages (Schulz et al., 2012). However, the exact contribution of YS macrophages versus fetal liver monocytes to LC and tissue macrophage homeostasis during adult life remains unclear. Our results together with our recent study on the embryonic origin of microglia clearly suggest that YS macrophage contribution to adult phagocytes varies between tissues.

For example, we recently found that the majority of adult microglia derive from E7.5 Runx1^{+} hematopoietic cells, whereas only a minor fraction of adult LCs derive from YS as the majority of YS-derived skin phagocytes are replaced by fetal liver monocyte–derived cells between E13.5 and E16.5. A similar scenario could apply to other tissue phagocytes during late embryogenesis. In addition, the contribution of YS primitive hematopoiesis to 8–12 wk-old adult tissue macrophages was significantly lower than that of microglia and LCs (Ginhoux et al., 2010). These results suggest that the contribution of YS primitive macrophages may decrease with time because of tissue macrophage turnover and replenishment from adult circulating precursors.

In summary, our findings identify LCs as an ontogenically distinct cell population among myeloid cells. The dual origin of LCs suggests that the LC differentiation program is not intrinsic to either YS macrophages or fetal liver monocytes, but rather depends on tissue-specific extrinsic factors that control the recruitment, differentiation, and homeostasis of LC precursors. Supporting this hypothesis is the fact that adult bone marrow monocytes also gave rise to epidermal LC precursors. Thus, the nature of the cell-extrinsic factors that control the recruitment and survival of the first wave of myeloid precursors remains to be determined. In addition, identifying cell-specific markers that discriminate YS- versus fetal liver–derived LCs may help uncover distinct immune function that may contribute to the maintenance of skin integrity.

MATERIALS AND METHODS

Mice. C57BL/6 (CD45.2[+]) mice, congenic C57BL/6 CD45.1[+] mice, *Cx3cr1*[gfp/+]C57BL/6 mice (Jung et al., 2000), and *Csf1r*[gfp/+]C57BL/6 mice (Macrophage Fas-induced apoptosis, MaFIA; Burnett et al., 2004) were purchased from the The Jackson Laboratory. *Csf1*[op/op] and *Csf1r*^{−/−} FVB/NJ mice were produced as previously described (Dai et al., 2002). C57BL/6 *Ncx-1*^{−/−} mice were generated as previously described (Koushik et al., 2001). All mice (7–8 wk old) were bred and kept under specific pathogen–free conditions in the Biomedical Resource Centre, Singapore. Embryonic development was estimated considering the day of vaginal plug observation as 0.5 d after conception. For activation experiments, *Runx1*[Cre/wt] (CD1 background; Center for Developmental Biology accession no. CDB0524K, available at http://www.cdb.riken.jp/arg/mutant%20mice%20list.html), *Rosa*[R26R-eYFP/R26R-eYFP], and *Rosa*[R26R-LacZ/R26R-LacZ] C57BL/6 mice were used as previously described (Samokhvalov et al., 2007). All experiments and procedures were approved by the Institutional Animal Care and Use Committee (IACUC), in accordance with the guidelines of the Agri-Food and Veterinary Authority (AVA) and the National Advisory Committee for Laboratory Animal Research (NACLAR).

Induction of cell tagging with 4'OHT. For the induction of cell tagging with 4'OHT (Sigma-Aldrich), 4'OHT solution was prepared as previously reported and administered by intraperitoneal injection (5–10 mg) to pregnant mice at 6.5–9.5 d after conception (Samokhvalov et al., 2007). As 4'OHT treatment during pregnancy interferes with normal delivery, to trace cells marked during embryogenesis into adulthood, caesarean sections were performed at term, and neonates were fostered by lactating females.

In vivo newborn reconstitution assays and in utero fetal liver monocyte adoptive transfer. For newborn reconstitution assays, CD45.2[+] C57BL/6 pups were sublethally irradiated in the first 24 h after birth (2× 300 rad, 3 h apart using a Caesium source) and reconstituted with 2 × 10^{6} bone marrow cells from CD45.1^{+} C57BL/6 mice, by injection in the liver using a 33-gauge needle (Hamilton). For adoptive transfer experiments, monocytes (DAPI^{−}CD45^{+}CD11b^{+}F4/80^{+}) were sorted on a FACSAria II (BD) from the fetal liver of time-mated E13.5–E14.5 C57BL/6 CD45.1^{+} embryos. Sorted cells reached >98% purity after post-sort verification, and were adoptively transferred in utero into the peritoneal cavity of time-mated E13.5–E14.5 C57BL/6 CD45.2[+] host embryos (2–3 × 10^{5} cells per embryo) as previously described (Chan et al., 2007). In brief, a full-depth midline laparotomy was performed to expose the gravid uterus. Identification of the fetal abdomen through the translucent uterine wall allowed delivery of the monocytes by the intraperitoneal route. Cells were injected in 10 µl of saline using a 33-gauge needle, and the mice were allowed to recover in a warmed cage after closure of the abdominal wound with 6/0 silk sutures.

Cell suspension preparations. Skin cell suspensions were isolated as previously described (Ginhoux et al., 2007) and analyzed by flow cytometry. In brief, mouse ears (split in dorsal and ventral parts) or whole skin (starting from E16.5) were first incubated for 60 min in HBSS containing Dispase (2.4 mg/ml, working activity of 1.7 U/mg; Invitrogen) to allow for separation of dermal and epidermal sheets before subsequent Collagenase incubation. All tissues from adult mice, newborns, or embryos were cut into small pieces, incubated in HBSS containing 10% fetal bovine serum, and Collagenase type IV (0.2 mg/ml, working activity of 770 U/mg; Sigma-Aldrich; 2 h for adult tissues and 1 h for newborns and embryonic tissues), and then syringed through a 19-gauge needle to obtain a homogeneous cell suspension. Embryonic blood cells were collected after decapitation in PBS 10 mM EDTA and red blood cells were lysed. Analysis was performed by flow cytometry, gating on singlets of DAPI^{−} CD45^{+} cells.

Flow cytometry and cell cycle analysis. Flow cytometric studies were performed using a BD FACSCanto and a BD LSR II (BD) with subsequent data analysis using FlowJo software (Tree Star). Fluorochrome- or biotin-conjugated mAbs specific for mouse B220 (clone RA3-6B2), MHC class II I-A/I-E (clone M5/114.15.2), CD11b (clone M1/70), CD45 (clone 30F11), CD45.1 (clone A20), CD45.2 (clone 104), CSF-1R (clone AFS98), Gr-1Ly6C/G (clone RB6-8C5), and CD3 (clone 17A2), the corresponding isotype controls and the secondary reagents (allophycocyanin, peridinin chlorophyll protein, and phycoerythrin–indotricarbocyanine–conjugated streptavidin) were purchased either from BD or eBioscience. Anti-F4/80 (A3-1) mAb was purchased from Serotec. Polyclonal antibody to langerin (E17) was purchased from Santa Cruz Biotechnology, Inc. Intracellular staining against langerin was performed with the BD Cytofix/Cytoperm kit (BD) according to the manufacturer's protocol. For cell cycle analysis, stained cell suspensions were first fixed in 2% paraformaldehyde in PBS solution (30 min), and then washed and fixed in 70% ethanol (2 h). After washing, cells were incubated overnight with 10 mM DAPI in PBS solution to stain cell DNA content before data acquisition.

Immunohistochemistry analysis. Time-mated E12.5 and E16.5 *Cx3cr1*[gfp/+] embryos were fixed in 2% paraformaldehyde solution containing 30% sucrose overnight and snap-frozen in OCT. 20-µm frozen sections were labeled with biotinylated anti-F4/80 (Serotec) followed by Dy649-conjugated streptavidin (Jacksons ImmunoResearch Laboratories). Sections were counterstained with DAPI for nuclei staining and analyzed with a confocal microscope (FV-1000 confocal system; Olympus). For whole-mount X-Gal staining, embryos were dissected and fixed immediately in a solution containing 0.2% glutaraldehyde for 1 h on ice, washed three times at room temperature in a buffer containing 0.1% sodium deoxycholate and 0.02% NP-40, and stained with X-Gal at 37°C overnight.

Imaging procedures. For cytospin and SEM preparations, corresponding myeloid progenitors were sorted using a FACSAria II (BD) to achieve 98% purity. For cytospin, purified cells were spun onto glass slides, dried overnight, stained using the Hema 3 System (Thermo Fisher Scientific), and rinsed in distilled water. Images were analyzed using an Eclipse E800 microscope (Nikon) at a 10 × 60-fold magnification. For SEM imaging, sorted

cells were coated on a poly-lysine (Sigma-Aldrich) pretreated glass coverslip for 15 min at room temperature, fixed in 2.5% glutaraldehyde 0.1 M phosphate buffer for 1 h, pH 7.4, at room temperature and washed 2 times in PBS. After post-fixation with 1% osmium tetroxide (Ted Pella Inc.) at room temperature for 1 h, cells were washed in deionized water, dehydrated with a graded series of ethanol immersions starting at 25–100%, and critical point dried (CPD 030; Bal-Tec). The glass coverslip was then laid on an adhesive film on an SEM sample holder and firmly touched with an adhesive sample holder. The surface on which the cells were deposited and the adhesive surfaces were coated with 5 nm of platinum by sputter coating in a high-vacuum sputtering device (SCD005 sputter coater; Bal-Tec). The coated samples were examined with a field emission scanning electron microscope (JSM-6701F; JEOL) at an acceleration voltage of 8 kV using the in-lens secondary electron detector, with a working distance ranging from 7.5 to 8.3 mm. Magnification ×10,000, except for subepidermal mesenchyme LC precursors, which had a magnification of ×7,000 (Fig. 7). For multiphoton imaging of embryos, pregnant mice were euthanized by CO_2 asphyxiation, the $Cx3cr1^{gfp/+}$ or $Csf1^{gfp/+}$ embryos were isolated and mounted on a customized Petri dish for multiphoton imaging on a LaVision Biotec TrimScope equipped with a 20× water immersion objective. Evans blue was injected intravenously to label blood vessels. The whole intact embryo was incubated in DAPI for 5 min to label the surface of the skin to distinguish the exact localization of the cells in relation to the surface. For imaging, the explanted embryo was exposed to polarized laser light at a wavelength of 950 nm. Three-dimensional (x,y,z) image stacks of the skin in the vicinity of the upper limb were acquired (1-μm spacing in z-axis over a total distance of up to 130–160 μm). For static three-dimensional images of the embryonic skin at E12.5, embryos were positioned upright in Agarose gels. Acquired image stacks were processed using Imaris software (Bitplane).

Statistical analysis. For statistical analysis, repeated measures of ANOVA and Mann-Whitney tests (with a 95% confidence) were performed using Prism 4.0 (GraphPad Software). All p-values are two-tailed.

REFERENCES

Ajami, B., J.L. Bennett, C. Krieger, W. Tetzlaff, and F.M. Rossi. 2007. Local self-renewal can sustain CNS microglia maintenance and function throughout adult life. *Nat. Neurosci.* 10:1538–1543. http://dx.doi.org/10.1038/nn2014

Azoulay, M., C.G. Webb, and L. Sachs. 1987. Control of hematopoietic cell growth regulators during mouse fetal development. *Mol. Cell. Biol.* 7:3361–3364.

Bertrand, J.Y., A. Jalil, M. Klaine, S. Jung, A. Cumano, and I. Godin. 2005. Three pathways to mature macrophages in the early mouse yolk sac. *Blood.* 106:3004–3011. http://dx.doi.org/10.1182/blood-2005-02-0461

Bogunovic, M., F. Ginhoux, A. Wagers, M. Loubeau, L.M. Isola, L. Lubrano, V. Najfeld, R.G. Phelps, C. Grosskreutz, E. Scigliano, et al. 2006. Identification of a radio-resistant and cycling dermal dendritic cell population in mice and men. *J. Exp. Med.* 203:2627–2638. http://dx.doi.org/10.1084/jem.20060667

Breathnach, A.S., W.K. Silvers, J. Smith, and S. Heyner. 1968. Langerhans cells in mouse skin experimentally deprived of its neural crest component. *J. Invest. Dermatol.* 50:147–160.

Burnett, S.H., E.J. Kershen, J. Zhang, L. Zeng, S.C. Straley, A.M. Kaplan, and D.A. Cohen. 2004. Conditional macrophage ablation in transgenic mice expressing a Fas-based suicide gene. *J. Leukoc. Biol.* 75:612–623. http://dx.doi.org/10.1189/jlb.0903442

Chan, J., S.N. Waddington, K. O'Donoghue, H. Kurata, P.V. Guillot, C. Gotherstrom, M. Themis, J.E. Morgan, and N.M. Fisk. 2007. Widespread distribution and muscle differentiation of human fetal mesenchymal stem cells after intrauterine transplantation in dystrophic mdx mouse. *Stem Cells.* 25:875–884. http://dx.doi.org/10.1634/stemcells.2006-0694

Chang-Rodriguez, S., W. Hoetzenecker, C. Schwärzler, T. Biedermann, S. Saeland, and A. Elbe-Bürger. 2005. Fetal and neonatal murine skin harbors Langerhans cell precursors. *J. Leukoc. Biol.* 77:352–360. http://dx.doi.org/10.1189/jlb.1004584

Chorro, L., A. Sarde, M. Li, K.J. Woollard, P. Chambon, B. Malissen, A. Kissenpfennig, J.B. Barbaroux, R. Groves, and F. Geissmann. 2009. Langerhans cell (LC) proliferation mediates neonatal development, homeostasis, and inflammation-associated expansion of the epidermal LC network. *J. Exp. Med.* 206:3089–3100. http://dx.doi.org/10.1084/jem.20091586

Dai, X.M., G.R. Ryan, A.J. Hapel, M.G. Dominguez, R.G. Russell, S. Kapp, V. Sylvestre, and E.R. Stanley. 2002. Targeted disruption of the mouse colony-stimulating factor 1 receptor gene results in osteopetrosis, mononuclear phagocyte deficiency, increased primitive progenitor cell frequencies, and reproductive defects. *Blood.* 99:111–120. http://dx.doi.org/10.1182/blood.V99.1.111

Daneman, R., L. Zhou, A.A. Kebede, and B.A. Barres. 2010. Pericytes are required for blood-brain barrier integrity during embryogenesis. *Nature.* 468:562–566. http://dx.doi.org/10.1038/nature09513

Foster, C.A., K.A. Holbrook, and A.G. Farr. 1986. Ontogeny of Langerhans cells in human embryonic and fetal skin: expression of HLA-DR and OKT-6 determinants. *J. Invest. Dermatol.* 86:240–243. http://dx.doi.org/10.1111/1523-1747.ep12285201

Geissmann, F., M.G. Manz, S. Jung, M.H. Sieweke, M. Merad, and K. Ley. 2010. Development of monocytes, macrophages, and dendritic cells. *Science.* 327:656–661. http://dx.doi.org/10.1126/science.1178331

Ginhoux, F., and M. Merad. 2010. Ontogeny and homeostasis of Langerhans cells. *Immunol. Cell Biol.* 88:387–392. http://dx.doi.org/10.1038/icb.2010.38

Ginhoux, F., F. Tacke, V. Angeli, M. Bogunovic, M. Loubeau, X.M. Dai, E.R. Stanley, G.J. Randolph, and M. Merad. 2006. Langerhans cells arise from monocytes in vivo. *Nat. Immunol.* 7:265–273. http://dx.doi.org/10.1038/ni1307

Ginhoux, F., M.P. Collin, M. Bogunovic, M. Abel, M. Leboeuf, J. Helft, J. Ochando, A. Kissenpfennig, B. Malissen, M. Grisotto, et al. 2007. Blood-derived dermal langerin+ dendritic cells survey the skin in the steady state. *J. Exp. Med.* 204:3133–3146. http://dx.doi.org/10.1084/jem.20071733

Ginhoux, F., K. Liu, J. Helft, M. Bogunovic, M. Greter, D. Hashimoto, J. Price, N. Yin, J. Bromberg, S.A. Lira, et al. 2009. The origin and development of nonlymphoid tissue CD103+ DCs. *J. Exp. Med.* 206:3115–3130. http://dx.doi.org/10.1084/jem.20091756

Ginhoux, F., M. Greter, M. Leboeuf, S. Nandi, P. See, S. Gokhan, M.F. Mehler, S.J. Conway, L.G. Ng, E.R. Stanley, et al. 2010. Fate mapping analysis reveals that adult microglia derive from primitive macrophages. *Science.* 330:841–845. http://dx.doi.org/10.1126/science.1194637

Godin, I.E., J.A. Garcia-Porrero, A. Coutinho, F. Dieterlen-Lièvre, and M.A. Marcos. 1993. Para-aortic splanchnopleura from early mouse embryos contains B1a cell progenitors. *Nature.* 364:67–70. http://dx.doi.org/10.1038/364067a0

Holbrook, K.A., and G.F. Odland. 1975. The fine structure of developing human epidermis: light, scanning, and transmission electron microscopy of the periderm. *J. Invest. Dermatol.* 65:16–38. http://dx.doi.org/10.1111/1523-1747.ep12598029

Jung, S., J. Aliberti, P. Graemmel, M.J. Sunshine, G.W. Kreutzberg, A. Sher, and D.R. Littman. 2000. Analysis of fractalkine receptor

CX(3)CR1 function by targeted deletion and green fluorescent protein reporter gene insertion. *Mol. Cell. Biol.* 20:4106–4114. http://dx.doi .org/10.1128/MCB.20.11.4106-4114.2000

Kingston, D., M.A. Schmid, N. Onai, A. Obata-Onai, D. Baumjohann, and M.G. Manz. 2009. The concerted action of GM-CSF and Flt3-ligand on in vivo dendritic cell homeostasis. *Blood.* 114:835–843. http://dx.doi .org/10.1182/blood-2009-02-206318

Koushik, S.V., J. Wang, R. Rogers, D. Moskophidis, N.A. Lambert, T.L. Creazzo, and S.J. Conway. 2001. Targeted inactivation of the sodium-calcium exchanger (Ncx1) results in the lack of a heartbeat and abnormal myofibrillar organization. *FASEB J.* 15:1209–1211.

Kumaravelu, P., L. Hook, A.M. Morrison, J. Ure, S. Zhao, S. Zuyev, J. Ansell, and A. Medvinsky. 2002. Quantitative developmental anatomy of definitive haematopoietic stem cells/long-term repopulating units (HSC/RUs): role of the aorta-gonad-mesonephros (AGM) region and the yolk sac in colonisation of the mouse embryonic liver. *Development.* 129:4891–4899.

Lichanska, A.M., and D.A. Hume. 2000. Origins and functions of phagocytes in the embryo. *Exp. Hematol.* 28:601–611. http://dx.doi.org/ 10.1016/S0301-472X(00)00157-0

Lichanska, A.M., C.M. Browne, G.W. Henkel, K.M. Murphy, M.C. Ostrowski, S.R. McKercher, R.A. Maki, and D.A. Hume. 1999. Differentiation of the mononuclear phagocyte system during mouse embryogenesis: the role of transcription factor PU.1. *Blood.* 94:127–138.

Lin, H., E. Lee, K. Hestir, C. Leo, M. Huang, E. Bosch, R. Halenbeck, G. Wu, A. Zhou, D. Behrens, et al. 2008. Discovery of a cytokine and its receptor by functional screening of the extracellular proteome. *Science.* 320:807–811. http://dx.doi.org/10.1126/science.1154370

M'Boneko, V., and H.J. Merker. 1988. Development and morphology of the periderm of mouse embryos (days 9-12 of gestation). *Acta Anat. (Basel).* 133:325–336. http://dx.doi.org/10.1159/000146662

Medvinsky, A.L., N.L. Samoylina, A.M. Müller, and E.A. Dzierzak. 1993. An early pre-liver intraembryonic source of CFU-S in the developing mouse. *Nature.* 364:64–67. http://dx.doi.org/10.1038/364064a0

Merad, M., and M.G. Manz. 2009. Dendritic cell homeostasis. *Blood.* 113:3418–3427. http://dx.doi.org/10.1182/blood-2008-12-180646

Merad, M., M.G. Manz, H. Karsunky, A. Wagers, W. Peters, I. Charo, I.L. Weissman, J.G. Cyster, and E.G. Engleman. 2002. Langerhans cells renew in the skin throughout life under steady-state conditions. *Nat. Immunol.* 3:1135–1141. http://dx.doi.org/10.1038/ni852

Merad, M., F. Ginhoux, and M. Collin. 2008. Origin, homeostasis and function of Langerhans cells and other langerin-expressing dendritic cells. *Nat. Rev. Immunol.* 8:935–947. http://dx.doi.org/10.1038/nri2455

Mildner, A., H. Schmidt, M. Nitsche, D. Merkler, U.K. Hanisch, M. Mack, M. Heikenwalder, W. Brück, J. Priller, and M. Prinz. 2007. Microglia in the adult brain arise from Ly-6ChiCCR2+ monocytes only under defined host conditions. *Nat. Neurosci.* 10:1544–1553. http://dx.doi.org/10.1038/nn2015

Moore, M.A., and D. Metcalf. 1970. Ontogeny of the haemopoietic system: yolk sac origin of in vivo and in vitro colony forming cells in the developing mouse embryo. *Br. J. Haematol.* 18:279–296. http://dx.doi .org/10.1111/j.1365-2141.1970.tb01443.x

Naito, M., K. Takahashi, and S. Nishikawa. 1990. Development, differentiation, and maturation of macrophages in the fetal mouse liver. *J. Leukoc. Biol.* 48:27–37.

North, T., T.L. Gu, T. Stacy, Q. Wang, L. Howard, M. Binder, M. Marín-Padilla, and N.A. Speck. 1999. Cbfa2 is required for the formation of intra-aortic hematopoietic clusters. *Development.* 126:2563–2575.

Orkin, S.H., and L.I. Zon. 2008. Hematopoiesis: an evolving paradigm for stem cell biology. *Cell.* 132:631–644. http://dx.doi.org/10.1016/ j.cell.2008.01.025

Palis, J., S. Robertson, M. Kennedy, C. Wall, and G. Keller. 1999. Development of erythroid and myeloid progenitors in the yolk sac and embryo proper of the mouse. *Development.* 126:5073–5084.

Rae, F., K. Woods, T. Sasmono, N. Campanale, D. Taylor, D.A. Ovchinnikov, S.M. Grimmond, D.A. Hume, S.D. Ricardo, and M.H. Little. 2007. Characterisation and trophic functions of murine embryonic macrophages based upon the use of a Csf1r–EGFP transgene reporter. *Dev. Biol.* 308:232–246. http://dx.doi.org/10.1016/j.ydbio.2007.05.027

Reams, W.M. Jr., and S.P. Tompkins. 1973. A developmental study of murine epidermal Langerhans cells. *Dev. Biol.* 31:114–123. http://dx.doi .org/10.1016/0012-1606(73)90323-0

Romani, N., G. Schuler, and P. Fritsch. 1986. Ontogeny of Ia-positive and Thy-1-positive leukocytes of murine epidermis. *J. Invest. Dermatol.* 86:129–133. http://dx.doi.org/10.1111/1523-1747.ep12284135

Romani, N., B.E. Clausen, and P. Stoitzner. 2010. Langerhans cells and more: langerin-expressing dendritic cell subsets in the skin. *Immunol. Rev.* 234:120–141. http://dx.doi.org/10.1111/j.0105-2896.2009.00886.x

Samokhvalov, I.M., N.I. Samokhvalova, and S. Nishikawa. 2007. Cell tracing shows the contribution of the yolk sac to adult haematopoiesis. *Nature.* 446:1056–1061. http://dx.doi.org/10.1038/nature05725

Sato, N., S.K. Ahuja, M. Quinones, V. Kostecki, R.L. Reddick, P.C. Melby, W.A. Kuziel, and S.S. Ahuja. 2000. CC chemokine receptor (CCR)2 is required for langerhans cell migration and localization of T helper cell type 1 (Th1)-inducing dendritic cells. Absence of CCR2 shifts the Leishmania major–resistant phenotype to a susceptible state dominated by Th2 cytokines, b cell outgrowth, and sustained neutrophilic inflammation. *J. Exp. Med.* 192:205–218. http://dx.doi.org/10.1084/jem.192.2.205

Schulz, C., E. Gomez Perdiguero, L. Chorro, H. Szabo-Rogers, N. Cagnard, K. Kierdorf, M. Prinz, B. Wu, S.E. Jacobsen, J.W. Pollard, et al. 2012. A lineage of myeloid cells independent of Myb and hematopoietic stem cells. *Science.* 336:86–90. http://dx.doi.org/10.1126/ science.1219179

Schuster, C., C. Vaculik, C. Fiala, S. Meindl, O. Brandt, M. Imhof, G. Stingl, W. Eppel, and A. Elbe-Bürger. 2009. HLA-DR+ leukocytes acquire CD1 antigens in embryonic and fetal human skin and contain functional antigen-presenting cells. *J. Exp. Med.* 206:169–181. http:// dx.doi.org/10.1084/jem.20081747

Silvers, W.K. 1957. A histological and experimental approach to determine the relationship between gold-impregnated dendritic cells and melanocytes. *Am. J. Anat.* 100:225–239. http://dx.doi.org/10.1002/aja .1001000204

Takahashi, K., F. Yamamura, and M. Naito. 1989. Differentiation, maturation, and proliferation of macrophages in the mouse yolk sac: a light-microscopic, enzyme-cytochemical, immunohistochemical, and ultrastructural study. *J. Leukoc. Biol.* 45:87–96.

Takahashi, K., M. Naito, and L.D. Shultz. 1992. Differentiation of epidermal Langerhans cells in macrophage colony-stimulating-factor-deficient mice homozygous for the osteopetrosis (op) mutation. *J. Invest. Dermatol.* 99:46S–47S. http://dx.doi.org/10.1111/1523-1747.ep12668982

Tavian, M., and B. Péault. 2005. Embryonic development of the human hematopoietic system. *Int. J. Dev. Biol.* 49:243–250. http://dx.doi.org/ 10.1387/ijdb.041957mt

Tripp, C.H., S. Chang-Rodriguez, P. Stoitzner, S. Holzmann, H. Stössel, P. Douillard, S. Saeland, F. Koch, A. Elbe-Bürger, and N. Romani. 2004. Ontogeny of Langerin/CD207 expression in the epidermis of mice. *J. Invest. Dermatol.* 122:670–672. http://dx.doi.org/10.1111/j.0022-202X.2004.22337.x

Wei, S., S. Nandi, V. Chitu, Y.G. Yeung, W. Yu, M. Huang, L.T. Williams, H. Lin, and E.R. Stanley. 2010. Functional overlap but differential expression of CSF-1 and IL-34 in their CSF-1 receptor-mediated regulation of myeloid cells. *J. Leukoc. Biol.* 88:495–505. http://dx.doi .org/10.1189/jlb.1209822

Weiss, L.W., and A.S. Zelickson. 1975. Embryology of the epidermis: ultrastructural aspects. III. Maturation and primary appearance of dendritic cells in the mouse with mammalian comparisons. *Acta Derm. Venereol.* 55:431–442.

Witmer-Pack, M.D., D.A. Hughes, G. Schuler, L. Lawson, A. McWilliam, K. Inaba, R.M. Steinman, and S. Gordon. 1993. Identification of macrophages and dendritic cells in the osteopetrotic (op/op) mouse. *J. Cell Sci.* 104:1021–1029.

Yoshida, H., S. Hayashi, T. Kunisada, M. Ogawa, S. Nishikawa, H. Okamura, T. Sudo, L.D. Shultz, and S. Nishikawa. 1990. The murine mutation osteopetrosis is in the coding region of the macrophage colony stimulating factor gene. *Nature.* 345:442–444. http://dx.doi .org/10.1038/345442a0